Prevention of hypoxia by myoglobin expression in human tumor cells promotes differentiation and inhibits metastasis

Maria Galluzzo, Selma Pennacchietti, Stefania Rosano, Paolo M. Comoglio, and Paolo Michieli

Laboratory of Experimental Therapy, Institute for Cancer Research and Treatment, University of Turin Medical School, Turin, Italy.

As a tumor grows, it requires increased amounts of oxygen. However, the tumor blood vessels that form to meet this demand are functionally impaired, leading to regions of hypoxia within the tumor. Such hypoxia is one of the hallmarks of malignancy and is thought to promote a number of tumorigenic properties. Here, we sought to determine how tumors without hypoxia would progress by engineering A549 human lung carcinoma cells to ectopically express myoglobin (Mb), a multifunctional heme protein that specializes in oxygen transport, storage, and buffering. Mb expression prevented the hypoxic response in vitro and delayed tumor engraftment and reduced tumor growth following xenotransplantation into mice. Experimental tumors expressing Mb displayed reduced or no hypoxia, minimal HIF-1α levels, and a homogeneously low vessel density. Mb-mediated tumor oxygenation promoted differentiation of cancer cells and suppressed both local and distal metastatic spreading. These effects were primarily due to reduced tumor hypoxia, because they were not observed using point-mutated forms of myoglobin unable to bind oxygen and they were abrogated by expression of a constitutively active form of HIF-1α. Although limited to xenograft models, these data provide experimental proof of the concept that hypoxia is not just a side effect of deregulated growth but a key factor on which the tumor relies in order to promote its own expansion.

Introduction

Poor oxygenation is a common feature of solid tumors. On one hand, deregulated growth overrides the ability of the vasculature to adapt to the increased oxygen demand (1). On the other, tumor blood vessels are functionally impaired compared with normal tissues due to structural and biological abnormalities including tortuosity, leakiness, lack of pericytes, unhomogeneous distribution, and haphazard interconnection (2). As a result, neoplastic lesions often contain areas subject to acute or chronic hypoxia regardless of blood vessel proximity (3). Hypoxic niches may function as incubators for malignant evolution because they select, in a Darwinian manner, for more aggressive cancer cells (4). Furthermore, hypoxia induces a number of cellular adaptations that may turn advantageous during tumor progression, including a switch to anaerobic metabolism (5), increased genetic instability (6), promotion of angiogenesis (7), activation of invasive growth (8), and preservation of the stem state (9). Tumor hypoxia also represents a major obstacle for radiotherapy (10) and for some types of anticancer drugs that require oxygen to exert their pharmacological effect (11).

Although low tumor oxygenation is universally recognized as a hallmark of malignancy and despite the great knowledge that has been generated in the last few years on the pathophysiology of hypoxia, we still do not fully understand the role of cancer cell pO_2 in tumor onset and progression, nor can we tell its relevance as a therapeutic target. This is essentially due to the lack of an appropriate technology that allows modulation of tumor cell oxygenation in experimental models of cancer. The importance of protooncogenes in embryo development has been elucidated through the introduction of homologous recombination techniques. Likewise, target validation in cancer therapy has been made possible by the extension of RNA interference technology to mammalian systems. In the case of oxygen, an effective method that knocks out tumor hypoxia either in cell systems or in animals has not yet been developed. For this reason, no clear-cut experiment has been conducted that definitely asserts whether hypoxia is an epiphenomenon or drives malignant progression.

Indirect methods that aim at decreasing tumor hypoxia have actually been attempted in the past, including hyperbaric oxygen (12) and systemic erythropoietin treatment (13). However, both these approaches present conceptual weaknesses and practical drawbacks. On one hand, either method increases oxygen delivery to the whole organism and not the tumor only; on the other, it is uncertain whether increasing pO_2 systemically will result in enhanced oxygenation of a tumor that presents manifest delivery flaws, due to the above-discussed vascular abnormalities. Here, we present what we believe is a novel approach to target tumor hypoxia that is based on a genetic rather than an environmental principle and that overcomes both these limitations. Using lentiviral vector technology, we introduced the myoglobin (Mb) gene into cancer cells, thus allowing them to "breathe" even in a hypoxic environment. Following in vitro characterization, we injected them into experimental animals, thus generating tumor models that are functional "knockouts" of hypoxia.

Mb is a cytoplasmic heme protein that plays a well-characterized role in oxygen transport and free radical scavenging in skeletal and cardiac muscle cells (14, 15). Its oxygen-related functions are multiple and include at least 3 different activities. First, Mb acts as an oxygen reservoir, binding O_2 in aerobic conditions and releasing it under hypoxia (16). Second, Mb is capable of buffer-

Conflict of interest: The authors have declared that no conflict of interest exists.

Nonstandard abbreviations used: A.I., apoptotic index; Hb, hemoglobin; ICD, intercapillary distance; Mb, myoglobin; MLA, mean lumen area; MVD, microvascular density; P.I., proliferation index.

Citation for this article: *J. Clin. Invest.* **119**:865–875 (2009). doi:10.1172/JCI36579.

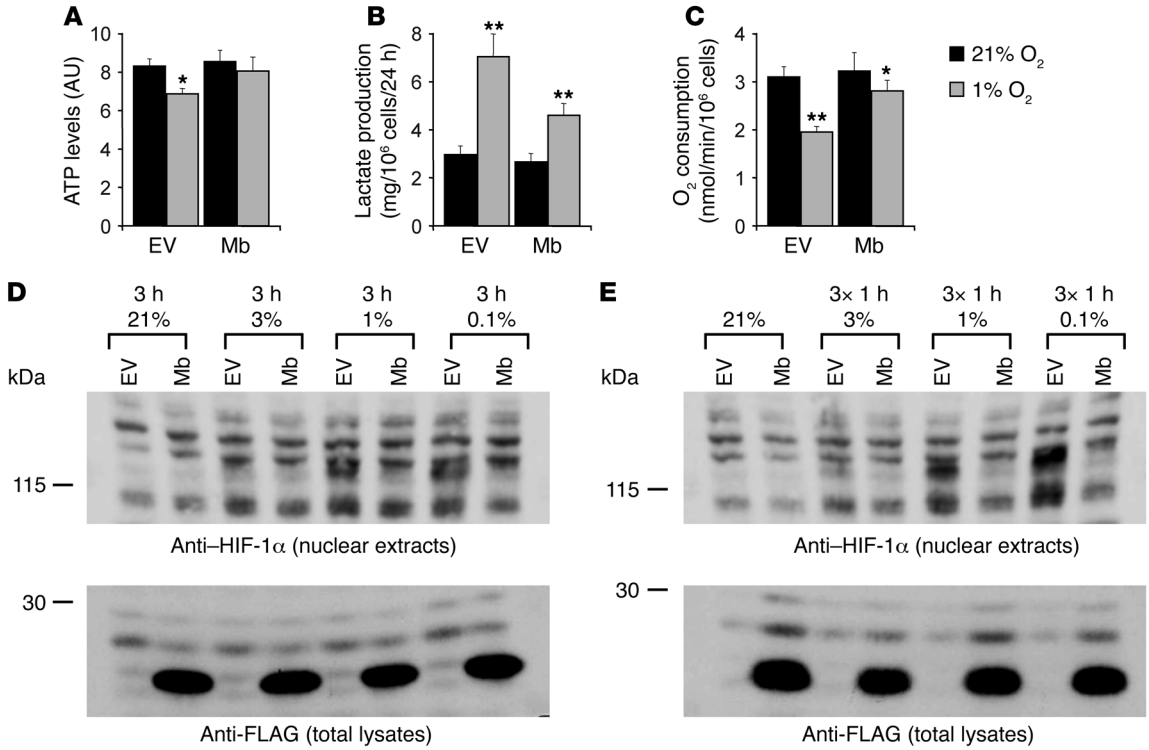

Figure 1
Mb expression attenuates the hypoxic response of cancer cells. (**A**) Lentiviral vector–transduced cells were incubated in normoxia (21% O_2) or hypoxia (1% O_2) for 24 hours, and intracellular ATP levels were determined on total cell lysates. Statistical significance was calculated between each experimental sample and the empty vector (EV) control at 21% O_2. *$P < 0.05$; **$P < 0.01$. (**B**) Cells were incubated in normoxia or hypoxia, and lactate concentration was determined in the conditioned medium. (**C**) Cells were incubated in normoxia or hypoxia and then resuspended in normoxic medium. Oxygen consumption was measured in a sealed chamber using a Clark-type electrode. (**D**) Cells were incubated at different pO_2 values for 3 hours, and HIF-1α levels were determined by Western blotting using anti–HIF-1α antibodies. (**E**) Cells were subjected to repeated cycles of hypoxia and reoxygenation (1 hour at 21%, 3%, 1%, or 0.1% O_2 followed by 30 minutes at 21% O_2, repeated 3 times), and HIF-1α levels were determined by Western blotting. Cells incubated at 21% O_2 were used as controls.

ing intracellular pO_2, playing a role similar to that of creatine phosphokinase in maintaining ATP concentration constant (17). Third, Mb supplements simple O_2 diffusion by working as a carrier in an activity known as facilitated O_2 diffusion (18, 19). Also, the scavenging functions of Mb are multiple and are related to at least 2 different classes of molecules. One includes NO, which competes with O_2 in cytochrome *c* oxidase binding, thus reducing mitochondrial respiration efficiency (20). The second class of molecules scavenged by Mb includes ROS, which plays an important role in oxidative stress on one hand and in cell signaling on the other (21). We reasoned that if cancer cells expressed a similar multifunctional oxygen transporter, the tumor as a whole would (a) capture more oxygen from blood vessels, (b) benefit from a more homogeneous oxygenation, and (c) be less subject to cycles of hypoxia and reoxygenation.

The data presented in this study demonstrate that our working hypothesis is well founded and suggest that Mb gene transfer is a valid method for studying the role of oxygen and oxygen species in tumor progression. We show that Mb expression does not alter the basic functions of cancer cells but allows them to utilize oxygen more efficiently during hypoxia, thus inhibiting HIF-1α stabilization and preventing the hypoxic response. In mouse models of cancer, Mb expression resulted in delayed tumor implantation, reduced xenograft growth, and minimal HIF-1α levels. Angiogenesis and invasion were strongly inhibited. These effects were not observed using point-mutated forms of Mb unable to bind oxygen but capable of scavenging free radicals. These effects were bypassed by a constitutively active form of HIF-1α. Mutant Mb expression actually resulted in promotion of tumor growth and metastasis, conceivably due to depletion of ROS. These data suggest that hypoxia is not just an epiphenomenon associated with deregulated growth but a key factor driving tumor progression. They also suggest that the pleiotropic functions of Mb affect cancer biology in multiple ways. While oxygen transport correlates with tumor suppression, protection against oxidative stress shows a relationship with tumor growth and invasion.

Results

Transferring the Mb gene into tumor cells. To experiment with a genetic approach to reducing tumor hypoxia, we transferred the *Mb* gene into tumor cells using lentiviral vector technology. The mouse *Mb* gene, obtained by RT-PCR amplification from skeletal muscle total RNA, was engineered into the lentiviral vector pRRLsin.PPT.CMV.Wpre, which displays enhanced gene transfer activity due to the presence of the HIV-1 PRE sequence (22). A FLAG epitope was engineered at the C terminus to allow protein immunodetection. A549 human lung carcinoma cells, which are an established model system for the analysis of tumor hypoxia (8), were first engi-

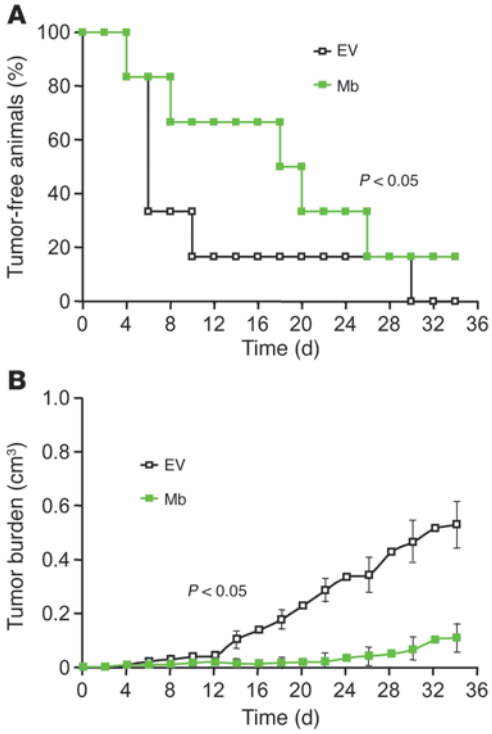

Figure 2
Mb expression inhibits tumor growth. Lentiviral vector–transduced A549 lung carcinoma cells were injected subcutaneously into CD1 *nu/nu* mice, and the formation of experimental tumors was monitored over time. (**A**) Kaplan-Meier–like analysis of tumor latency. Statistical significance was calculated comparing the median values. (**B**) Analysis of tumor volume. Statistical significance refers to the average values after day 20.

neered to express GFP to track metastatic dissemination and then transduced with the recombinant lentiviral vector encoding Mb or with an empty vector as a control. Mb expression in lentiviral-vector–transduced cells was analyzed by Western blotting using anti-Mb antibodies and anti-FLAG antibodies. Mouse skeletal muscle and heart protein extracts were used as controls. According to this analysis, the levels of Mb expression reached by lentiviral gene transfer approached those displayed by endogenous Mb in skeletal muscle (Supplemental Figure 1A; supplemental material available online with this article; doi:10.1172/JCI36579DS1). GFP expression was determined by Western blotting (Supplemental Figure 1A) and flow cytometry (not shown). As Mb is normally expressed in myocytes, we investigated to determine whether its ectopic expression in cancer cells could result in toxicity or affect their housekeeping functions in any way. To this end, we subjected lentiviral vector–transduced cells to a series of tests in vitro. First, we compared the growth rate of Mb-expressing tumor cells with that of empty vector–transduced control cells (Supplemental Figure 1B). Second, we measured the percentage of dead cells and the basal levels of apoptosis (Supplemental Figure 1C). Third, we determined DNA synthesis in the absence or presence of serum growth factors (Supplemental Figure 1D). As no significant difference between the 2 populations could be detected in any of the assays performed, we concluded that Mb expression does not alter the basic biology of cancer cells.

Mb expression sustains cancer cell oxygenation during hypoxia. We next analyzed the metabolic profiles of lentiviral vector–transduced cells under normoxic and hypoxic conditions. To this end, we incubated cells in 21% O_2 or 1% O_2 and then measured (a) ATP levels (in the cell) and (b) lactate production (in the medium). Using a Clark electrode, we also determined (c) oxygen consumption (in a sealed chamber). This analysis revealed that A549 carcinoma cells produce high basal levels of lactate even in normoxia (approximately 3 mg/10^6 cells/24 h), typical of a Warburg effect. However, lactate levels did increase about 3 times when cells were incubated in hypoxia. This was accompanied by a slight reduction in ATP levels (approximately 17%) and a drop in O_2 consumption (approximately 37%). Mb expression resulted in an attenuated metabolic change following oxygen depletion: in fact, under hypoxia, Mb-expressing cells displayed reduced lactate production (Figure 1A), sustained oxygen consumption (Figure 1B), and increased ATP production (Figure 1C) compared with control cells. This is consistent with the idea that Mb functions as an oxygen supplier when environmental pO_2 is low, thus allowing cells to maintain an aerobic metabolism or at least reducing their shift toward glycolysis. Since the majority of cellular adaptations to hypoxia are mediated by stabilization of HIF-1α, we analyzed HIF-1α levels under normoxic and hypoxic conditions in both Mb-expressing and control cells. Cells were incubated in decreasing oxygen concentrations (21%, 3%, 1%, and 0.1% O_2), and HIF-1α expression was determined by Western blotting on nuclear extracts. As a control, Mb expression was determined on total lysates using anti-FLAG antibodies. Consistent with the idea that Mb sustains cancer cell oxygenation in a hypoxic environment, this analysis revealed that Mb-expressing cells maintain lower levels of HIF-1α compared with control cells when exposed to hypoxia (Figure 1D). This effect is even more dramatic when intermittent, short cycles of hypoxia and reoxygenation are applied instead of continuous hypoxia (Figure 1E). These results suggest that Mb attenuates the hypoxic response of cancer cells by enhancing their oxygenation during hypoxia and allowing them to "hold their breath" for short periods of time.

Mb expression facilitates oxygen diffusion in 3D cultures. To analyze the ability of Mb to promote oxygen transport in a context closer to that of a real tissue, we seeded preformed, tumor-like spheroids containing approximately 1,000 lentiviral vector–transduced cells into a Matrigel layer (Supplemental Figure 2A). Following stabilization in normoxic conditions, the environmental pO_2 was lowered to 5%. Hypoxic spheroids were incubated with the hypoxia marker pimonidazole hydrochloride (23), fixed, embedded in paraffin, and then processed for analysis. Spheroid oxygenation was analyzed by immunohistochemistry using anti-pimonidazole antibodies. Spheroid sections of similar size were compared for their staining intensity and pattern. This analysis revealed that, while control colonies displayed a hypoxic gradient culminating in a necrotic core typical of a diffusion-limited oxygen supply, spheroids expressing Mb had no necrotic areas and were overall less hypoxic (Supplemental Figure 2B). Although pimonidazole staining only indirectly reflects tissue hypoxia, these results are consistent with a role for Mb in facilitating O_2 diffusion and suggest that Mb expression in tissue-like cell agglomerates results in a more homogeneous oxygenation.

Mb expression inhibits tumor growth. We next analyzed the effect of Mb expression in vivo. Lentiviral vector–transduced cells were injected subcutaneously into CD1 *nu/nu* mice, and the formation

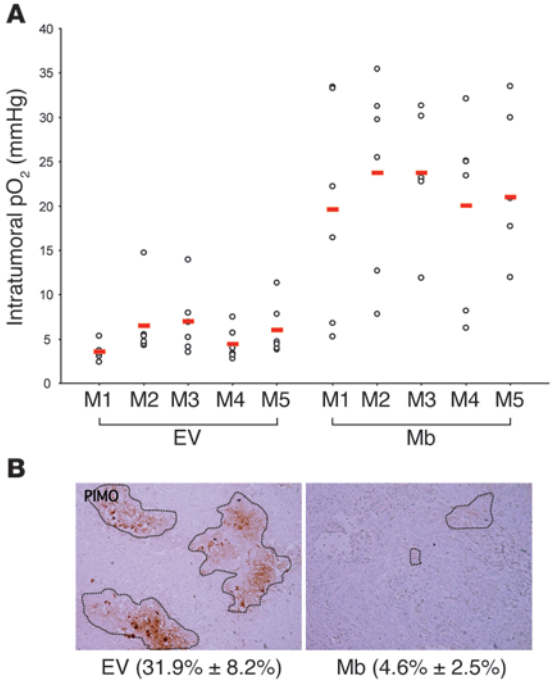

Figure 3
Mb expression promotes tumor oxygenation. (**A**) Approximately 5 weeks after tumor cell injection, intratumoral pO_2 was measured directly using a ruthenium probe. At least 6 distinct measurements in different tumor locations were performed for each mouse. Red bars indicate average values. M1, mouse 1. (**B**) Following i.p. injection of pimonidazole hydrochloride, mice were euthanized and tumors extracted for analysis. The extent of tumor hypoxia was determined by immunohistochemical analysis of tumor sections using anti-pimonidazole (PIMO) antibodies. Hypoxia was quantified by calculating the percentage of pimonidazole-positive area (identified by the dotted outlines) over the total area (mean ± SD; in parentheses). Original magnification, ×100.

of experimental tumors was monitored over time. As shown by the Kaplan-Meier–like analysis in Figure 2A, 50% of control mice bore a visible tumor by day 6. In contrast, mice injected with cells expressing Mb required 18 days to reach the same percentage. Following tumor engraftment, tumors expressing Mb grew more slowly than control tumors and had a more regular, spherical shape. After 5 weeks, control mice had an average tumor burden 4.8 times larger than mice of the Mb group (Figure 2B). Analysis of tumor weight yielded similar results (not shown). Consistent with the notion that hypoxia stimulates the tumor to "nest" in the host organism, these results suggest that Mb expression in cancer cells delays tumor implantation and growth.

Mb expression promotes tumor oxygenation. At about 5 weeks after cell injection, the actual oxygen concentration in experimental tumors was determined by fluorescence quenching using an intratumoral optical fiber. This technique exploits the ability of O_2 in solution to quench fluorescence emitted by a ruthenium probe and allows direct measurement of tissue pO_2 in vivo (24). By inserting the probe in multiple tumor sites, we determined the mean intratumoral pO_2 of Mb-expressing as well as control tumors. The results of this analysis are shown in Figure 3A. On average, tumors expressing Mb displayed an oxygen concentration about 4 times higher than that of controls; in fact, the mean pO_2 value of control tumors was 5.5 ± 2.7 mmHg (approximately 0.7% O_2), while that of Mb tumors measured 21.62 ± 9.9 mmHg (approximately 3.0% O_2). Subcutaneous insertion of the ruthenium probe into a CD1 *nu/nu* mouse without tumor resulted in a mean pO_2 value of 30.9 mmHg (approximately 4.1% O_2), thus suggesting that experimental tumors are less efficiently oxygenated than the hypodermis itself. Following pO_2 measurement, mice were injected with pimonidazole hydrochloride, euthanized, and subjected to autopsy. The degree of tumor hypoxia was further characterized by immunohistochemical analysis of tumor sections using anti-pimonidazole antibodies. This technique revealed that control tumors were riddled with hypoxic areas of different size and intensity, typical of a highly disorganized growth. In contrast and consistent with our direct pO_2 measurements using fluorescence quenching, Mb-expressing tumors contained very few hypoxic regions and none of high intensity. The extent of tumor hypoxia was quantified by determining the percentage of pimonidazole-positive area over the total area analyzed. According to this quantification, control tumors contained approximately 7 times more hypoxic areas than Mb-expressing tumors (Figure 3B).

Mb expression results in lower HIF-1α levels. The expression of endogenous markers of hypoxia was also examined. Tumor sections were analyzed by immunofluorescence using anti HIF-1α antibodies. Several sections per tumor were scrutinized by microscopy, and the number of HIF-1α–positive cells per microscopic field was scored. This analysis revealed that tumors expressing Mb contained remarkably fewer HIF-1α–positive cells than control tumors (approximately 10 times; Supplemental Figure 3A). HIF-1α, however, is a hypoxia marker with a very short half-life that dissolves very quickly following reoxygenation. To obtain a better picture of both transient and chronic hypoxia, we therefore stained tumor sections with anti–carbonic anhydrase IX (anti-CAIX) antibodies. CAIX is a transmembrane protein involved in pH homeostasis, the expression of which is regulated by HIF-1, but its long half-life lets it persist for a longer time after reoxygenation (25). Consistent with the results obtained by anti-pimonidazole immunostaining and anti–HIF-1α immunofluorescence, this analysis revealed that a significantly larger area of control tumors was subjected to hypoxia than tumors expressing Mb (Supplemental Figure 3B).

Mb expression inhibits tumor angiogenesis. Immunofluorescence staining of tumor sections using antibodies directed against the CD31 endothelial marker provided more insights into the biological activity of Mb. Control tumors were characterized by a chaotic angiogenesis; highly vascularized regions were randomly alternated with necrotic regions (Figure 4A). In vital parts of the tumor, microvascular density (MVD) (Figure 4B) was high (202 ± 46 vessels/mm^2), while intercapillary distance (ICD) (Figure 4C) was low (72 ± 7.7 μm). Vessel size, measured as mean lumen area (MLA) (Figure 4D), was extremely variable (2,345 ± 4,285 μm^2). In contrast, Mb-expressing tumors had a more organized architecture. Vessels were concentrated around the tumor, while MVD within the neoplastic mass was very low (49 ± 20 vessels/mm^2). Consistent with a role of Mb in facilitated O_2 diffusion, ICD was homogeneously high (155 ± 43.0 μm) and vessels of large size — typical of hypoxic tissues — were absent (MLA, 247 ± 262 μm^2). Interestingly, muscle tissues in Mb-deficient mice or in Antarctic icefishes lacking Mb also display increased vessel density and

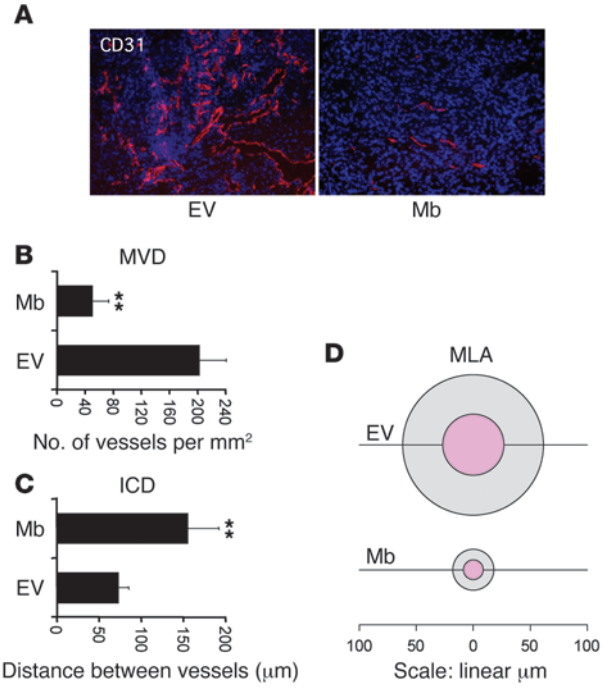

Figure 4
Mb expression inhibits tumor angiogenesis. (**A**) Immunofluorescence analysis of tumor vessels using anti-CD31 antibodies (red). Nuclei are stained with DAPI (blue). Original magnification, ×100. (**B**) Analysis of MVD. Statistical significance refers to the difference between the empty vector and Mb groups. $^{**}P < 0.01$. (**C**) Analysis of intercapillary distance (ICD). (**D**) MLA of tumor vessels. The mean value is indicated by the inner (pink) circle. The outer circle indicates SD. The linear scale refers to mean vessel diameter.

size compared with their Mb-expressing counterparts (26, 27). This change in vessel number and diameter represents an adaptive response of the tissue aimed at compensating for reduced oxygen diffusion and storage.

Mb expression promotes tumor cell differentiation. Histological analysis of tumor sections revealed that control tumors contained several necrotic areas and had a highly disorganized, anaplastic phenotype. In contrast, tumors expressing Mb were less necrotic and were organized in well-differentiated, gland-like structures (Figure 5). Mb-expressing tumors were also riddled with hollow structures containing a PAS/Alcian-positive secretion, similar to those observed in normal mouse lungs (see inset). As A549 tumor cells originate from type II pneumocytes, which are deputed to pulmonary surfactant secretion, these results suggest that Mb-mediated tumor oxygenation reverts the oncogenic phenotype of A549 cells by inducing their differentiation or — alternatively — that a more oxygenated environment selects for cells that are more prone to differentiate. Either way, this observation provides further support to the notion that hypoxia preserves tumor cell stemness and undifferentiated state (9, 28).

Mb expression reduces tumor cell proliferation and death. To determine the effect of Mb-mediated tumor oxygenation on cancer cell proliferation, tumor sections were further characterized by immunohistochemistry using antibodies against the Ki67 mitotic marker (Supplemental Figure 4A). Consistent with the observation that Mb promotes tumor cell differentiation, Mb-expressing tumors displayed a very low proliferation index (P.I.) (0.175 ± 0.062) compared with controls (P.I., 0.372 ± 0.028). We also determined cancer cell apoptosis using the TUNEL method (Supplemental Figure 4B). Consistent with a more oxygenated environment and a reduced tissue necrosis associated with Mb expression, this analysis revealed that tumors expressing Mb had a lower apoptotic index (A.I.) (0.024 ± 0.018) compared with control tumors (A.I., 0.163 ± 0.059). Representative images of Ki67 and TUNEL staining are shown in Supplemental Figure 4C.

Mb expression inhibits invasion and metastasis. Hypoxia represents a fundamental environmental stimulus that promotes tumor invasion and metastasis. We therefore determined whether Mb expression in the primary tumor affected local lymph node invasion and spontaneous metastasis to the lung in our mouse model. Local invasion was determined on inguinal lymph node sections by immunohistochemical analysis using anti-GFP antibodies. As shown in Figure 6A, GFP-positive cells could be identified in the lymph nodes from mice with control tumors (75.6 ± 11.5 cells/field) but not in those from mice bearing Mb-expressing tumors (0.6 ± 1.3 cells/field). Pulmonary metastatic colonization was determined by real-time analysis of genomic DNA extracted from lungs using a *gfp*-specific TaqMan probe. As shown in Figure 6B, lungs of the empty vector group contained 8.7 times more metastatic cells than lungs of the Mb group. Immunohistochemical analysis of lung sections using anti-GFP antibodies confirmed these data (Figure 6C). Therefore, Mb-mediated tumor oxygenation results in decreased invasion and metastasis. However, since Mb expression inhibits tumor growth, we cannot rule out that reduced metastasis is due to smaller size of the primary lesions. To address this issue, we compared the extent of metastatic lung colonization in mice bearing tumors of comparable volume (approximately 0.2 cm^3) regardless of the time required to reach such volume. In this setting as well, the content of *gfp* DNA in lungs was greater in control mice compared with mice of the Mb group (Figure 6D), thus suggesting that "breathing" cancer cells are less prone to "escape" from the tumor, independent of its size.

Constitutive HIF-1α expression bypasses Mb-mediated tumor suppression. To determine whether the biological effects consequent to Mb overexpression were actually mediated by reduced HIF-1α expression, we engineered a mutated, constitutively active form of HIF-1α in which both prolines 402 and 564, targets of prolyl hydroxylase enzymes, are substituted with alanines. Mutant HIF-1α was expressed in A549 cells by lentiviral vector technology alone or in combination with Mb. Cells expressing Mb alone, mutant HIF-1α alone, or a combination of Mb plus mutant HIF-1α (Supplemental Figure 5A) were injected subcutaneously into CD1 *nu/nu* mice along with control cells, and the formation of experimental tumors was monitored over time. After approximately 5 weeks, animals were euthanized and tumors extracted for analysis. This analysis revealed that HIF-1α constitutive expression abrogated Mb-mediated tumor suppression as measured by tumor burden (Supplemental Figure 5B), tumor angiogenesis (Supplemental Figure 5C), and number of pulmonary metastases (Supplemental Figure 5D). Interestingly, tumors expressing Mb and mutant HIF-1α did not show the same differentiated phenotype observed for tumors expressing Mb only (Supplemental Figure 5E), suggesting that HIF-1α overexpression bypasses Mb-mediated cancer cell differentiation in this system.

Engineering mutant forms of Mb unable to bind oxygen. As mentioned in the Introduction, Mb is not only an O_2 transporter but also a free radical scavenger. To dissect its multiple functions and to deter-

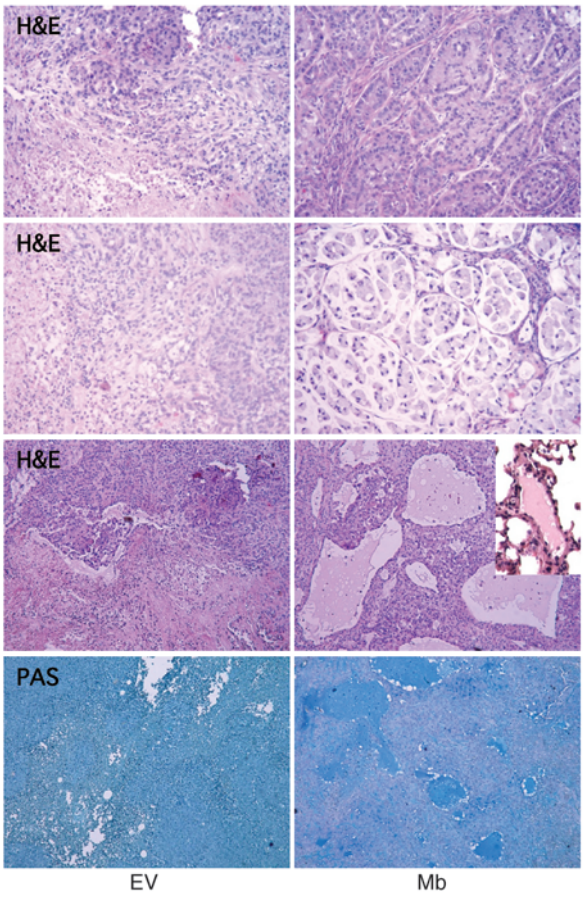

Figure 5
Mb expression promotes tumor differentiation. Rows 1–3, tumor sections were stained with H&E. Original magnification, ×100 (rows 1 and 2); ×50 (row 3). Inset shows histological preparation from a normal mouse lung. Original magnification, ×200. Row 4, tumor sections were stained with PAS–Alcian blue. Original magnification, ×50.

mine whether the biological effects of Mb overexpression are specific to its oxygen transport activity, we engineered a series of mutants that were impaired in their ability to bind O_2. For designing these mutants, we took advantage of the naturally occurring mutations that target hemoglobin (Hb) and are responsible for reduced systemic oxygen transport in human methemoglobinemia disorders (29). In fact, Hb and Mb share a high degree of structural and functional homology (Figure 7A). In both Hb and Mb, 2 key residues positioned on opposite sides of the heme plan determine oxygen binding: the proximal histidine (also referred to as the eighth amino acid of the F helix or F8) and the distal histidine (also referred to as the seventh amino acid of the E helix or E7). Both the F8 and the E7 histidines are essential for oxygen transport and are targets of inactivating mutations in hereditary methemoglobinemia. In the first Mb mutant, we substituted the proximal histidine (His94 in the mouse Mb protein) with a tyrosine residue. In the second mutant, we substituted both the proximal histidine and the distal histidine (His65 in the mouse Mb protein) with an alanine residue. These substitutions are known to result in stabilization of the ferric form of heme iron (Fe^{3+}), thus yielding to a constitutive met-Mb which is unable to bind oxygen but is potentially capable of performing scavenging reactions (30–32). The mutant forms of Mb were engineered into the pRRLsin.PPT.CMV.Wpre lentiviral vector and then expressed in A549 cells. Expression of wild-type and mutant Mb in lentiviral vector–transduced cells was analyzed by Western blotting using anti-FLAG antibodies (Figure 7B). All forms of Mb reached similar expression levels. Intriguingly, both His(F8)Tyr and His(E7)Ala/His(F8)Ala mutants displayed an electromobility shift compared with wild-type Mb, conceivably due to a change in conformation. Cells expressing mutant Mb grew at the same rate as control cells or cells expressing wild-type Mb (Figure 7C). However, cells expressing His(F8)Tyr and His(E7)Ala/His(F8)Ala Mb displayed increased ROS scavenging activity compared with cells expressing wild-type Mb (Supplemental Figure 6A). This can be explained by reduced steric hindrance around the active pocket of the mutant proteins and by the fact that, while O_2 binding requires Fe^{2+}, most scavenging reactions entail Fe^{3+} (30). In NO scavenging assays performed using a chemical NO donor, cells expressing His(F8)Tyr Mb displayed reduced activity compared with wild-type Mb (Supplemental Figure 6B). This is consistent with the notion that oxy-Mb has higher affinity for NO than met-Mb. However, cells expressing His(E7)Ala/His(F8)Ala Mb scavenged NO almost as efficiently as wild-type Mb, confirming that substitution of the distal histidine with an apolar amino acid dramatically increases the binding rate of met-Mb for NO (32).

The ability of Mb to inhibit tumor growth and metastasis depends on oxygen transport. The ability of mutant Mb to inhibit tumor growth and metastasis was analyzed by the same in vivo assays described above for wild-type Mb. In brief, lentiviral vector–transduced cells were injected subcutaneously into CD1 *nu/nu* mice, and tumor formation was monitored over time. After approximately 1 month, intratumoral pO_2 was measured as above, and then mice were euthanized. Tumors were extracted for analysis and lungs analyzed for the presence of metastatic cells. The results of this analysis are summarized in Table 1. In terms of tumor latency, wild-type Mb was the only form of Mb that delayed tumor implantation. No significant effect was observed with either mutant protein. Tumors expressing mutant Mb displayed a mean intratumoral pO_2 value indistinguishable from that of control tumors; only wild-type Mb could increase tumor oxygenation in this system. Consistent with this, HIF-1α levels decreased only in wild-type Mb–expressing tumors. Similarly, tumor angiogenesis was significantly reduced in tumors expressing wild-type Mb but not in tumors expressing His(F8)Tyr or His(E7)Ala/His(F8)Ala Mb. Finally, expression of wild-type Mb but not mutant Mb resulted in reduced tumor weight and in decreased metastatic spreading. Together, these data suggest that the antineoplastic and antiinvasive activity of Mb depends on its ability to transport O_2 and not to scavenge free radicals. Interestingly and somehow also unexpectedly, expression of His(F8)Tyr Mb or His(E7)Ala/His(F8)Ala Mb actually promoted tumor growth and invasion, conceivably because these proteins — while not capable of reducing hypoxia — protect cancer cells against oxidative stress.

Mb inhibits tumor growth and metastasis in orthotopic models. The ability of wild-type Mb to inhibit metastatic spreading was further assayed in 2 orthotopic mouse models of cancer and in 2 different experimental metastasis systems. MDA-MB-435-HGF human melanoma cells (33), TSA mouse mammary carcinoma cells, FG-2 human pancreatic carcinoma cells, and A549 human lung carcinoma cells were transduced with lentiviral vectors expressing wild-type or mutant (His[E7]Ala/His[F8]Ala) Mb as well as with an empty vector as control. Mb expression was determined by Western blot analysis

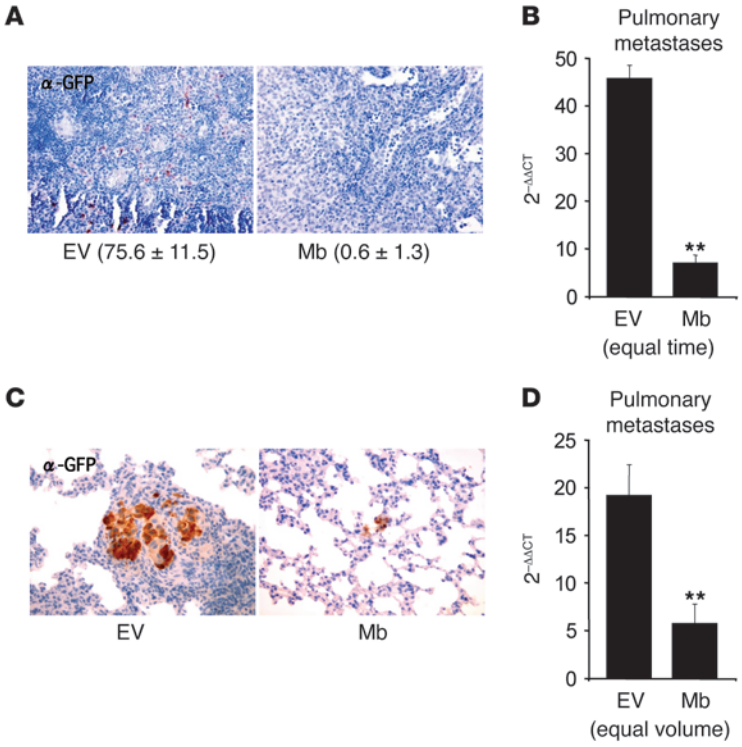

Figure 6
Mb expression inhibits metastatic spreading of tumor cells. (**A**) Inguinal lymph node invasion was determined by immunohistochemical analysis of lymph node sections using anti-GFP antibodies. Values in parentheses refer to the number of GFP-positive cells per field analyzed (mean ± SD). Original magnification, ×200. (**B**) The amount of *gfp* DNA present in lungs was determined by TaqMan analysis of lung genomic DNA. Values are expressed as $2^{-\Delta\Delta CT}$ using lung genomic DNA from a tumor-free mouse as reference sample. (**C**) Immunohistochemical analysis of lung sections using anti-GFP antibodies. A representative image for each group is shown. Original magnification, ×200. (**D**) Lung metastasis was determined as in **B** in mice bearing tumors of equal size (approximately 0.2 cm^3). $^{**}P < 0.01$.

using anti-FLAG antibodies (not shown). MDA-MB-435-HGF melanoma cells were injected underneath the skin of CD1 *nu/nu* mice. TSA mouse mammary carcinoma cells were injected into the mammary fat pad of syngeneic mice (BALB/c). Mice were monitored for tumor formation and autopsied when experimental tumors reached a volume of approximately 0.8 cm^2. FG-2 pancreatic carcinoma cells were injected into the peritoneal cavity of CD1 *nu/nu* mice, and mice were autopsied for the presence of abdominal colonies after 1 month. A549 lung carcinoma cells were injected in the tail veins of CD1 *nu/nu* mice, and animals were autopsied for the presence of pulmonary colonies after 1 month. The results of this analysis, summarized in Supplemental Table 1, identify a clear-cut dieresis between spontaneous and experimental metastases. In fact, wild-type Mb expression resulted in delayed tumor engraftment and in reduced metastatic spreading in the orthotopic models of spontaneous metastasis (MDA-MB-435-HGF and TSA) but did not have any effect on the formation of experimental metastases (FG-2 and A549). In contrast, mutant Mb promoted tumor growth and dissemination in all models analyzed.

Discussion

The present study seeks an answer to a fundamental question in cancer biology: is hypoxia a side effect of neoplastic growth or a key component of a pathological program that drives tumor progression and leads transformed cells to the metastatic route? We addressed this question by introducing into cancer cells a gene encoding an oxygen transporter, and we evaluated the biological consequences of this genetic manipulation in mouse models of cancer. The data presented here are not conclusive but provide support for a causative rather than epiphenomenal role of hypoxia in malignant evolution. Furthermore, they indicate that the pleiotropic activities of Mb profoundly affect tumor biology in multiple fashions.

Ectopic Mb expression did not alter the basic biology of cancer cells, thus ruling out that the biological effects consequent to its overexpression are due to toxicity. Cells expressing Mb displayed an enhanced ability to maintain an aerobic metabolism under hypoxia, thus suggesting that the ectopically expressed protein is fully functional. Mb expression inhibited hypoxia-induced HIF-1α stabilization under different pO_2 conditions. This is consistent with its ability to transport oxygen, but given the importance of free radicals in HIF-1α hydroxylation (34, 35), we cannot rule out a contribution of its ROS and NO scavenging activities as well. In any case, tumor spheroids expressing Mb showed a more homogeneous oxygenation and presented no central necrosis, suggesting that Mb does facilitate oxygen diffusion in this system.

In our in vivo experiments, Mb expression significantly delayed cancer cell engraftment and inhibited tumor growth. This is consistent with the idea that cancer cells exploit hypoxic signals to promote tumor "nesting." When tumor cells are transferred from the Petri dish into the hypodermis of a mouse, they reasonably get exposed to a hypoxic shock. Hypoxia stimulates the recruitment of endothelial cells from the host and the migration of cancer cells toward existing vessels, thus promoting the formation of a functional tumor mass composed of cancer cells as well as supporting host cells. If tumor cells do not sense hypoxia at the time of injection, they may fail to activate neoangiogenesis and invasion, thus ultimately delaying tumor engraftment. However, Mb expression also inhibited tumor growth once experimental tumors had appeared. As discussed, this may not be due to a toxic effect of Mb. Tumor inhibition is more likely to result from the ability of Mb to promote cancer cell differentiation. Since hypoxia inhibits cancer stem cell differentiation (9, 28) and Mb-expressing tumors displayed a higher pO_2 value, we can hypothesize that this effect is due to the ability of Mb to reduce the formation of hypoxic niches. From our experiments, however, it is not possible to tell whether

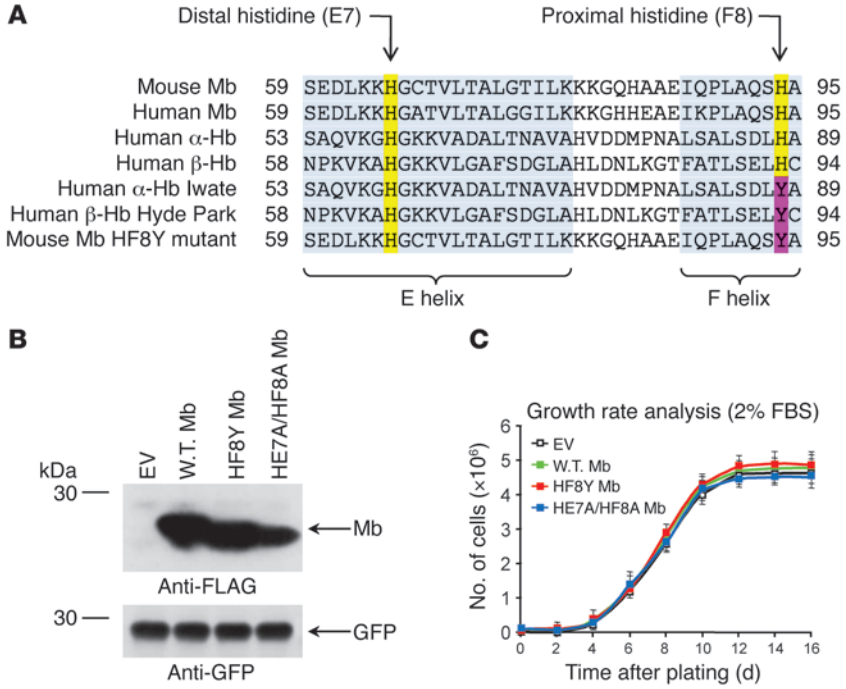

Figure 7
Engineering mutant forms of Mb unable to bind oxygen. (**A**) Alignment of helices E and F of mouse Mb, human Mb, human α-Hb (α-Hb), and human β-Hb (β-Hb). Iwate α-Hb and Hyde Park β-Hb are naturally occurring human Hb M mutants unable to transport O_2. Mouse HF8Y Mb is one of the Mb mutants used in this study. Numbers refer to the amino acid positions occupied by the first and last residues shown within the respective protein sequence. (**B**) Western blot analysis of A549 cells expressing wild-type or mutant Mb using anti-FLAG antibodies. Cells were also engineered to express GFP to track metastatic dissemination. HF8Y Mb, His(F8)Tyr Mb mutant; HE7A/HF8A Mb, His(F8)Ala/His(E7)Ala double mutant. (**C**) Growth rate analysis of lentiviral vector–transduced cells in the presence of 2% FBS.

increased intratumoral pO_2 is directly due to Mb-mediated oxygen transport or results from the tumors being smaller. In any case, it is interesting to note that highly differentiated tissues naturally expressing Mb including heart and skeletal muscles are less prone to developing malignancies compared with other organs without Mb. It is also noteworthy that a close relative of Mb with a broader range of expression, cytoglobin, behaves as a tumor suppressor in breast and lung carcinomas (36).

Mb expression also dramatically reduced tumor angiogenesis, though it promoted a more homogeneous oxygenation of cancer cells. In other words, experimental tumors expressing Mb were less hypoxic despite the fact that they displayed reduced MVD and increased intercapillary distance. Conversely, control tumors were riddled with several hypoxic areas despite their extensive vascularization. This may appear in contrast to common wisdom but can actually be explained when one considers 2 key issues. First, cancer cells expressing Mb need fewer vessels than regular cells because they "extract" oxygen more effectively from the environment and have a more efficient respiratory chain. Second, Mb-expressing tumors display a more ordered, "normalized" vasculature than control tumors, which are characterized by random and heterogeneous angiogenesis. A tumor with a normalized vasculature contains fewer vessels, but their increased functionality guarantees better tissue oxygenation (37). Multiple Mb activities may contribute to this phenotype, including its ability to transport oxygen and to scavenge NO.

Mb-mediated tumor oxygenation also resulted in reduced local invasion and decreased spontaneous metastasis. This cannot be due to reduced tumor size because Mb expression suppressed metastatic spreading even in mice bearing tumors of the same volume. Interestingly, Mb expression inhibited spontaneous metastasis (i.e., secondary colonies originating from cells that escape spontaneously from the primary lesion) in a variety of mouse models of cancer but did not have any effect on experimental metastasis (i.e., metastatic colonies arising from tumor cells injected systemically). These findings suggest that hypoxia plays a key role in the spreading of cancer cells from the primary tumor but is not involved in determining the ability of metastatic cells to form secondary colonies once these cells have reached systemic distribution. Other factors including resistance to anoikis and expression of specific homing markers conceivably determine the fate of the wandering cell. In this view, a putative antihypoxic therapy may work best as an adjuvant protocol but will not be effective in targeting preexisting metastases.

In this study, Mb was used as a biotechnological tool to prevent tumor hypoxia in experimental systems. However, as discussed, Mb is not only an oxygen transporter but also a free radical scavenger. To dissect these activities, we have mutagenized key amino acids in the active site of Mb. His(F8)Tyr Mb does not bind O_2 because heme iron is in the ferric form. This eases the entry of competitive ligands including peroxides and superoxides. Symmetrically, His(E7)Ala/His(F8)Ala Mb has insufficient specificity for O_2 because of reduced steric/charge hindrance, thus allowing noncanonical ligands to enter the active pocket and to oxidize heme iron. In both cases, free radical scavenging is favored at the expenses of oxygen transport. Thus, the data presented here should be interpreted keeping in mind that the 2 Mb mutants cannot bind O_2 but display enhanced ROS scavenging activity. We believe that this gain of function is responsible for increased tumor growth and metastasis. In fact, free radicals have a dual role in cancer biology: on one hand, they represent signaling molecules for oncogenic pathways; on the other, they cause damage to several cell components. Transformed cells with activated oncogenes display higher oxidative stress compared with normal cells and therefore need to set in motion cellular devices that reduce cell damage. Consistent with a detoxifying role of mutant Mb, tumors expressing His(F8)Tyr Mb or His(E7)Ala/His(F8)Ala Mb displayed a much lower A.I. and a higher P.I. compared with control tumors.

It should be noted that mutant forms of Mb unable to bind O_2 also lose their NO oxygenase activity. In fact, oxy-Mb is known to scavenge biologically active NO by the reaction $(Fe^{2+})\ MbO_2 + NO \rightarrow (Fe^{3+})\ Mb + NO^{3-}$. Indeed, His(F8)Tyr Mb did not scavenge

Table 1
The ability of Mb to inhibit tumor growth and metastasis depends on O_2 transport

	Redox status of heme Fe	Median A549 tumor latency (d)	Mean intratumoral pO_2 (mmHg)	HIF-1α expression (cells/field)	MVD (vs/mm²)	Mean A549 tumor weight (mg)	Spontaneous A549 metastases ($2^{-\Delta\Delta CT}$)
Empty vector	NA	6	5.5 ± 2.7	73 ± 21	202 ± 46	791 ± 161	45.6 ± 1.6
Wild-type Mb	Fe^{2+}	18	21.6 ± 9.9	7 ± 3	49 ± 20	163 ± 41	5.2 ± 3.3
HF8Y Mb	Fe^{3+}	6	5.4 ± 2.9	85 ± 26	199 ± 37	1,089 ± 321	77.4 ± 14.4
HE7A/HF8A Mb	Fe^{3+}	6	5.1 ± 3.1	71 ± 19	216 ± 32	1,107 ± 297	103.2 ± 17.9

The activity of wild-type Mb is compared with that of mutant Mb in mouse tumorigenesis assays using lentiviral vector–transduced A549 cells. Tumor latency is the lag time required by cells injected into a mouse to give rise to a palpable tumor. Intratumoral pO_2 was determined by fluorescence quenching and is the mean of 6 distinct measurements per mouse. HIF-1α expression was determined by immunofluorescence on frozen tumor sections and is expressed as the number of HIF-1α–positive cells per microscopic field analyzed. Mean tumor vessel density is the number of CD31-positive vessels per mm² of tumor section. Tumor weight refers to the wet weight of experimental tumors immediately following resection. Metastases were quantified by TaqMan analysis of *gfp* gene content in lung genomic DNA. For more detailed information, please refer to Methods. HF8Y Mb, His(F8)Tyr Mb mutant; HE7A/HF8A Mb, His(F8)Ala/His(E7)Ala double mutant.

NO in our cell-based assay. However, His(E7)Ala/His(F8)Ala Mb did perform well in the same assay because it can scavenge NO through a different, O_2-independent stochiometric mechanism. In light of these results, it is unlikely that the biological effects described in this study are exclusively due to Mb-mediated NO scavenging. It is more reasonable to propose instead that they are primarily mediated by the ability of Mb to transport oxygen and that depletion of NO — one of the most potent competitors of O_2 in several reactions — helps potentiate this effect.

The ability of Mb to reduce or prevent tumor hypoxia in experimental systems underscores a fundamental connection between cancer cell metabolism and tumor progression. Mb is a heme protein specifically evolved to increase the efficiency of oxidative phosphorylation in contracting muscle fibers. In this process, O_2 functions as the final electron acceptor of the mitochondrial electron transport chain (complexes I–IV). Each step of this transport results in proton pumping into the mitochondrial cytosol, leading to the formation of a proton gradient between the intermembrane space and the matrix. The proton gradient is used by the ATP synthase complex to generate ATP. The whole process is rather efficient, but some electron may "leak" out of the transport chain and be the cause of ROS generation. During hypoxia, a condition that is characterized by shortage of the final electron acceptor (O_2), electron leakiness increases dramatically, thus resulting in higher ROS levels. An increase in cellular ROS has several effects, including oxidation of Fe^{2+} to Fe^{3+}. Ferrous iron is used as a cofactor by enzymes of the prolyl hydroxylase family, which are responsible for hydroxylation of HIF-1α and thus its degradation by the proteasome. During hypoxia, ROS-mediated iron oxidation leads to HIF-1α stabilization and thus to the activation of the hypoxic response (38).

In this scenario, Mb functions as a supplier of oxygen during hypoxia. Its affinity for the O_2 molecule — at the conditions found in tissues — is intermediate between that of Hb and that of cytochrome *c* oxidase (the last component of the mitochondrial respiratory chain). Hence, Mb captures O_2 from the extracellular space and delivers it to the mitochondria. It cannot deliver it directly to prolyl hydroxylases because their affinity for oxygen is too low (39). Nevertheless, Mb ended up by decreasing HIF-1α levels in our experimental tumors, conceivably because it kept oxidative phosphorylation working even under low pO_2, thus preventing ROS formation during hypoxia. Indeed, this is what happens in contracting muscles: Mb extends the pO_2 window in which oxidative phosphorylation can occur efficiently, thus preventing the hypoxic response. In this view, the data presented here suggest that increasing the respiration efficiency of cancer cells — in some ways in contrast to common wisdom — is potentially beneficial from a therapeutic viewpoint because it prevents them from sensing hypoxia and thus activating adaptive responses that foster and support tumor progression. This is good news from a pharmacological perspective because oxidative phosphorylation can potentially be helped out by molecular means different than simply increasing oxygen concentration, including adenosine phosphate analogs, tricarbossilic acid cycle components, and inducible NO synthase inhibitors. Furthermore, most if not all components of the oxidative phosphorylation chain become tyrosine phosphorylated in response to growth factor and hormone stimuli (40), thus suggesting the possibility of modulating their activity by acting upstream along known signal transduction pathways.

Methods

Plasmid engineering. Mouse Mb cDNA was obtained by RT-PCR using mouse skeletal muscle total RNA as template. Total RNA was extracted from the musculus vastus medialis of a CD1 mouse (Charles River) using RNAwiz reagent (Ambion; Applied Biosystems) as suggested by the manufacturer. The following oligonucleotides were used as primers: Mb sense, 5′-GGATCCGCCACCATGGCTAGCGGGCTCAGTGATGGGGAGTGGCAG-3′; Mb antisense, 5′-TACAAGGAGCTAGGCTTCCAGGGCCTGCAGTGAGTCGAC-3′.

The nucleotide sequence of the amplicon corresponds to NCBI nucleotide sequence number BC025172 from base 168 to base 626. The 5′ and 3′ regions contain artificial restriction sites (embedded in the primer sequences) to facilitate subcloning and engineering. For antibody detection, a sequence coding for a double (repeated in tandem) FLAG epitope (SDYKDDDDKSDYKDDDDK) was inserted at the 3′ end, prior to the stop codon. Mutagenesis of the proximal and distal histidine was performed by standard PCR and genetic engineering techniques. The mutagenized residues correspond to His65 (distal histidine) and His94 (proximal histidine) in the mouse Mb protein. Alignment of globin sequences was performed using ClustalW software (http://www.ebi.ac.uk/Tools/clustalw2/index.html). The sequences compared correspond to (GenBank accession numbers): mouse Mb, BC025172; human Mb, BC014547; human α-Hb, BC101848; and human β-Hb, BC007075. Wild-type and mutant *Mb* cDNAs were subcloned into the BamHI-SalI restriction sites of the lentiviral vector pRRLsin.PPT.CMV.Wpre.

GFP in place of the *gfp* cDNA (22). Mutant HIF-1α was obtained by standard PCR and genetic engineering techniques using wild-type HIF-1α cDNA (NCBI nucleotide sequence number U22431) as template. The mutagenized cDNA, resulting in substitution of both Pro402 and Pro564 to Ala, was subcloned into the same lentiviral backbone using the BamHI-XhoI restriction sites. Human HGF cDNA (NCBII nucleotide sequence number M73239) was also subcloned into the pRRL lentiviral vector as described (33).

Cell cultures and lentiviral vectors. A549 human lung carcinoma cells obtained from ATCC (LGC Standards) were maintained in RPMI supplemented with 1% glutamine and 10% FBS (Sigma-Aldrich). TSA mouse breast carcinoma cells, obtained from Istituto Ortopedico Rizzoli, Bologna, Italy, were maintained in DMEM supplemented with 1% glutamine and 10% FBS (Sigma-Aldrich). FG-2 human pancreatic carcinoma cells (a gift of Vito Quaranta, Scripps Research Institute, La Jolla, California, USA) were maintained in RPMI supplemented with 1% glutamine and 10% FBS (Sigma-Aldrich). MDA-MB-435-HGF cells were obtained by transducing MDA-MB-435 human melanoma cells (obtained from the Georgetown University Tissue Culture Shared Resource, Washington, D.C., USA) with the above-described lentiviral vector encoding human HGF (33). Manipulation of O_2 atmosphere was achieved using a Ruskinn Invivo$_2$ 400 Hypoxic Workstation (0.1%–21% O_2; Biotrace, 3M) and a HERAcell 240 CO_2/O_2 Incubator (1%–21% O_2; Heraeus). Lentiviral vector stocks were produced by transient transfection as previously described (41). Viral p24 antigen concentration was determined by the HIV-1 p24 core profile ELISA kit (NEN Life Science Products) according to the manufacturer's instructions. Cells were transduced in 6-well plates (10^5 cells/well in 2 ml of medium) using 40 ng/ml of p24 in the presence of 8 μg/ml polybrene (Sigma-Aldrich) as described (41). Cells (including MDA-MB-345-HGF) were first transduced with the pRRLsin.PPT.CMV.Wpre.GFP plasmid (22), sorted to homogeneity using a BD FACSCalibur cell sorter (BD Biosciences), and then transduced with the appropriate lentiviral vector (empty vector, wild-type or mutant Mb, mutant HIF-1α). Mb expression was determined by Western blotting using polyclonal anti-Mb antibodies (Santa Cruz Biotechnology Inc.) and monoclonal anti-FLAG antibodies (Sigma-Aldrich). HIF-1α expression was analyzed by Western blotting using monoclonal anti–HIF-1α antibodies (BD Biosciences).

Tumorigenesis and spontaneous metastasis analysis. All animal procedures were approved by the Ethical Commission of the University of Turin and by the Italian Ministry of Health. Lentiviral vector–transduced A549 lung carcinoma cells (4×10^6 cells/mouse) were injected subcutaneously into the right posterior flanks of 6-week-old immunodeficient *nu/nu* female mice on a Swiss CD1 background (6 mice/group; Charles River). Tumor formation was monitored every 2 days, and tumor volume was calculated as described (42). At the end of the observation period, mice were injected i.p. with 60 mg/kg pimonidazole hydrochloride (Chemicon, Millipore) and then euthanized by CO_2 inhalation. Tumors were weighed and divided into 2 equal parts. One part was embedded in paraffin and processed for histological analysis; the other was embedded in Tissue-Tek OCT compound (Sakura Finetek) and immediately frozen in liquid nitrogen. Lungs were also divided into 2 parts; one was frozen in liquid nitrogen for DNA extraction and the other was embedded in paraffin as above. Lentiviral vector–transduced MDA-MB-435-HGF melanoma cells (3×10^6 cells/mouse) were injected subcutaneously into immunodeficient mice as above (6 mice/group). When tumors reached a volume of approximately 0.8 cm^3, mice were euthanized and lungs were frozen in liquid nitrogen for DNA extraction. Lentiviral vector–transduced TSA mammary carcinoma cells (5×10^5 cells/mouse) were injected into the mammary fat pad of 6-week-old syngeneic BALB/c female mice (6 mice/group; Charles River). When tumors reached a volume of approximately 0.8 cm^3, mice were euthanized and lungs were injected with India ink through the trachea to highlight metastases. Lungs were analyzed using a stereoscopic microscope.

Statistics. For all statistical analyses, a 2-tailed homoscedastic Student's *t* test was used. All values are expressed as mean ± SD. $P < 0.05$ was considered significant. For details, see Supplemental Methods.

Supplemental methods. For all experimental procedures not described here, please refer to the online Supplemental Methods section.

Acknowledgments

We thank Mauro Risio for histological analysis, Silvia Pastorekova for anti-CAIX antibodies, Luigi Naldini for lentiviral technology expertise, and Vittorio Modigliani for his generous and continuous support to Maria Galluzzo. This work has been supported in part by the Italian Association for Cancer Research (AIRC), the European Commission (FP7-HEALTH-2007-A grant 201640), the Compagnia San Paolo di Torino Foundation, the Cassa di Risparmio di Torino Foundation, and the Italian Ministry of University and Research.

Received for publication June 24, 2008, and accepted in revised form February 18, 2009.

Address correspondence to: Paolo Michieli, Institute for Cancer Research and Treatment (IRCC), Laboratory of Experimental Therapy, University of Turin Medical School, Strada Provinciale 142, km 3.95, I-10060 Candiolo, Turin, Italy. Phone: 39-011-993-3219; Fax: 39-011-993-3225; E-mail: paolo.michieli@ircc.it.

1. Brahimi-Horn, M.C., Chiche, J., and Pouysségur, J. 2007. Hypoxia and cancer. *J. Mol. Med.* **85**:1301–1307.
2. Jain, R.K. 2005. Normalization of tumor vasculature: an emerging concept in antiangiogenic therapy. *Science.* **307**:58–62.
3. Harris, A.L. 2002. Hypoxia — a key regulatory factor in tumour growth. *Nat. Rev. Cancer.* **2**:38–47.
4. Graeber, T.G., et al. 1996. Hypoxia-mediated selection of cells with diminished apoptotic potential in solid tumours. *Nature.* **379**:88–91.
5. Kim, J.W., Tchernyshyov, I., Semenza, G.L., and Dang, C.V. 2006. HIF-1-mediated expression of pyruvate dehydrogenase kinase: a metabolic switch required for cellular adaptation to hypoxia. *Cell Metab.* **3**:177–185.
6. Bindra, R.S., et al. 2005. Alterations in DNA repair gene expression under hypoxia: elucidating the mechanisms of hypoxia-induced genetic instability. *Ann. N. Y. Acad. Sci.* **1059**:184–195.
7. Tang, N., et al. 2004. Loss of HIF-1alpha in endothelial cells disrupts a hypoxia-driven VEGF autocrine loop necessary for tumorigenesis. *Cancer Cell.* **6**:485–495.
8. Pennacchietti, S., et al. 2003. Hypoxia promotes invasive growth by transcriptional activation of the met protooncogene. *Cancer Cell.* **3**:347–361.
9. Gustafsson, M.V., et al. 2005. Hypoxia requires notch signaling to maintain the undifferentiated cell state. *Dev. Cell.* **9**:617–628.
10. Trédan, O., Galmarini, C.M., Patel, K., and Tannock, I.F. 2007. Drug resistance and the solid tumor microenvironment. *J. Natl. Cancer Inst.* **99**:1441–1454.
11. Vaupel, P. 2004. Tumor microenvironmental physiology and its implications for radiation oncology. *Semin. Radiat. Oncol.* **14**:198–206.
12. Daruwalla, J., and Christophi, C. 2006. Hyperbaric oxygen therapy for malignancy: a review. *World J. Surg.* **30**:2112–2131.
13. Engert, A. 2005. Recombinant human erythropoietin in oncology: current status and further developments. *Ann. Oncol.* **16**:1584–1595.
14. Wittenberg, J.B., and Wittenberg, B.A. 2003. Myoglobin function reassessed. *J. Exp. Biol.* **206**:2011–2020.
15. Ordway, G.A., and Garry, D.J. 2004. Myoglobin: an essential hemoprotein in striated muscle. *J. Exp. Biol.* **207**:3441–3446.
16. Kooyman, G.L., and Ponganis, P.J. 1998. The physiological basis of diving to depth: birds and mammals. *Annu. Rev. Physiol.* **60**:19–32.
17. Hochachka, P.W. 1999. The metabolic implications of intracellular circulation. *Proc. Natl. Acad. Sci. U. S. A.* **96**:12233–12239.
18. Conley, K.E., and Jones, C. 1996. Myoglobin content and oxygen diffusion: model analysis of horse and steer muscle. *Am. J. Physiol.* **271**:C2027–C2036.
19. Merx, M.W., et al. 2001. Myoglobin facilitates oxygen diffusion. *FASEB J.* **15**:1077–1079.
20. Flögel, U., Merx, M.W., Gödecke, A., Decking, U.K., and Schrader, J. 2001. Myoglobin: A scavenger of bio-

active NO. *Proc. Natl. Acad. Sci. U. S. A.* **98**:735–740.
21. Flögel, U., Gödecke, A., Klotz, L.O., and Schrader, J. 2004. Role of myoglobin in the antioxidant defense of the heart. *FASEB J.* **18**:1156–1158.
22. Follenzi, A., Ailles, L.E., Bakovic, S., Geuna, M., and Naldini, L. 2000. Gene transfer by lentiviral vectors is limited by nuclear translocation and rescued by HIV-1 pol sequences. *Nat. Genet.* **25**:217–222.
23. Ljungkvist, A.S., Bussink, J., Kaanders, J.H., and van der Kogel, A.J. 2007. Dynamics of tumor hypoxia measured with bioreductive hypoxic cell markers. *Radiat. Res.* **167**:127–145.
24. Griffiths, J.R., and Robinson, S.P. 1999. The OxyLite: a fibre-optic oxygen sensor. *Br. J. Radiol.* **72**:627–630.
25. Kopacek, J., et al. 2005. MAPK pathway contributes to density- and hypoxia-induced expression of the tumor-associated carbonic anhydrase IX. *Biochim. Biophys. Acta.* **1729**:41–49.
26. Gödecke, A., et al. 1999. Disruption of myoglobin in mice induces multiple compensatory mechanisms. *Proc. Natl. Acad. Sci. U. S. A.* **96**:10495–10500.
27. Sidell, B.D., and O'Brien, K.M. 2006. When bad things happen to good fish: the loss of hemoglobin and myoglobin expression in Antarctic icefishes. *J. Exp. Biol.* **209**:1791–1802.
28. Axelson, H., Fredlund, E., Ovenberger, M., Landberg, G., and Pahlman, S. 2005. Hypoxia-induced dedifferentiation of tumor cells — a mechanism behind heterogeneity and aggressiveness of solid tumors. *Semin. Cell Dev. Biol.* **16**:554–563.
29. Percy, M.J., McFerran, N.V., and Lappin, T.R. 2005. Disorders of oxidised haemoglobin. *Blood Rev.* **19**:61–68.
30. Adachi, S., et al. 1993. Roles of proximal ligand in heme proteins: replacement of proximal histidine of human myoglobin with cysteine and tyrosine by site-directed mutagenesis as models for P-450, chloroperoxidase, and catalase. *Biochemistry.* **32**:241–252.
31. Ozaki, S.I., Roach, M.P., Matsui, T., and Watanabe, Y. 2001. Investigations of the roles of the distal heme environment and the proximal heme iron ligand in peroxide activation by heme enzymes via molecular engineering of myoglobin. *Acc. Chem. Res.* **34**:818–825.
32. Eich, R.F., et al. 1996. Mechanism of NO-induced oxidation of myoglobin and hemoglobin. *Biochemistry.* **35**:6976–6983.
33. Michieli, P., et al. 2004. Targeting the tumor and its microenvironment by a dual-function decoy Met receptor. *Cancer Cell.* **6**:61–73.
34. Bell, E.L., and Chandel, N.S. 2007. Mitochondrial oxygen sensing: regulation of hypoxia-inducible factor by mitochondrial generated reactive oxygen species. *Essays Biochem.* **43**:17–27.
35. Quintero, M., Brennan, P.A., Thomas, G.J., and Moncada, S. 2006. Nitric oxide is a factor in the stabilization of hypoxia-inducible factor-1alpha in cancer: role of free radical formation. *Cancer Res.* **66**:770–774.
36. Shivapurkar, N., et al. 2008. Cytoglobin, the newest member of the globin family, functions as a tumor suppressor gene. *Cancer Res.* **68**:7448–7456.
37. Fukumura, D., and Jain, R.K. 2007. Tumor microvasculature and microenvironment: targets for anti-angiogenesis and normalization. *Microvasc. Res.* **74**:72–84.
38. Kaelin, W.G., Jr. 2005. ROS: really involved in oxygen sensing. *Cell Metab.* **1**:357–358.
39. Semenza, G.L. 2001. HIF-1, O_2, and the 3 PHDs: how animal cells signal hypoxia to the nucleus. *Cell.* **107**:1–3.
40. Hüttemann, M., Lee, I., Samavati, L., Yu, H., and Doan, J.W. 2007. Regulation of mitochondrial oxidative phosphorylation through cell signaling. *Biochim. Biophys. Acta.* **1773**:1701–1720.
41. Vigna, E., and Naldini, L. 2000. Lentiviral vectors: excellent tools for experimental gene transfer and promising candidates for gene therapy. *J. Gene Med.* **2**:308–316.
42. Mazzone, M., et al. 2004. An uncleavable form of pro-scatter factor suppresses tumor growth and dissemination in mice. *J. Clin. Invest.* **114**:1418–1432.